Simulation-free estimation of an individual-based SEIR model for evaluating nonpharmaceutical interventions with an application to COVID-19 in Iowa

Daniel K. Sewell*[1], Aaron Miller [2], for the CDC MInD-Healthcare Program

1 Department of Biostatistics, University of Iowa, Iowa City, IA, USA
2 Department of Epidemiology, University of Iowa, Iowa City, IA, USA

Abstract

The ongoing COVID-19 pandemic has overwhelmingly demonstrated the need to accurately evaluate the effects of implementing new or altering existing nonpharmaceutical interventions. Since these interventions applied at the societal level cannot be evaluated through traditional experimental means, public health officials and other decision makers must rely on statistical and mathematical epidemiological models. Nonpharmaceutical interventions are typically focused on contacts between members of a population, and yet most epidemiological models rely on homogeneous mixing which has repeatedly been shown to be an unrealistic representation of contact patterns. An alternative approach is individual based models (IBMs), but these are often time intensive and computationally expensive to implement, requiring a high degree of expertise and computational resources. More often, decision makers need to know the effects of potential public policy decisions in a very short time window using limited resources. This paper presents an estimation algorithm for an IBM designed to evaluate nonpharmaceutical interventions. By utilizing recursive relationships, our method can quickly compute the expected epidemiological outcomes even for large populations based on any arbitrary contact network. We utilize our methods to evaluate the effects of various mitigation measures in Iowa, USA, at various times and to various degrees. `R` code for our method is provided in the supplementary material, thereby allowing others to utilize our approach for other regions.

Introduction

In December 2019, severe acute respiratory syndrome coronavirus 2 (SARS-CoV-2), was discovered in Wuhan China [1]. The virus causes the Coronavirus Disease 2019 (COVID-19), characterized by fever, cough, shortness of breath and other respiratory or flu-like symptoms. Severe cases can lead to pneumonia, respiratory failure, multi-organ dysfunction and death [2–4]. Since its discovery, the virus has rapidly moved across the globe and in March 11th, 2020 the World Health Organization declared COVID-19 to be a global pandemic. To date, over 5.6 million cases and over 350,000 deaths have been reported worldwide [5]. Nearly all countries have identified COVID-19 cases, with over 110 countries reporting greater than a thousand cases and 27 countries having recorded over a thousand deaths [5]. As the size of the pandemic continues to grow experts expect COVID-19 will pose a significant threat for many months and potentially years. Thus, the burden not just to population health, but also the overall healthcare system, skilled and long-term care, and the global economy are likely to be substantial.

Given the rapid growth with which COVID-19 has moved across the globe, policy makers have sought guidance to slow the spread, reduce the severity of the epidemic, or guide strategies for reopening. Consequently, many infectious disease models have been developed to forecast the trajectory of the current epidemic and to understand the likely impact of a range of interventions [6–15]. Models designed to capture certain aspects of the epidemic (e.g., forecasting mortality) may not be well suited for others (e.g., evaluating policy decision making), and so decision makers have increasingly had to navigate a range of diverse modeling approaches while attempting to find approaches that can meet the specific nature of a given setting [16]. In short, decision makers need information on the effects of public policy measures on an epidemic that is both timely and accurate. From a modeler's perspective, this translates into a model which is both computationally efficient and which captures salient features of transmission through a population.

One model which has received much attention from decision makers (e.g., [17]) is that of the Institute for Health Metrics and Evaluation (IHME) [6]. The IHME model, as of April 27, 2020, is a curve fitting approach which makes forecasts based on mortality rates over time. Curve fitting approaches, however, do not model transmission nor individual actors and settings, and thus have limited use to decision makers weighing whether to implement or relax nonpharmaceutical interventions.

Many other models have been developed that model disease transmission, but these too often rely on the assumption of homogeneous mixing, or mass action. For example, [7] implemented an early forecast for COVID-19 in Hubei, China, using a mass action compartmental model; [18] developed a compartmental model with homogeneous mixing which was used to capture the undocumented cases of COVID-19; [19] used a compartmental model with homogeneous mixing which allowed for time-varying reproduction number; and two web-based forecasting platforms [8, 9]. Some approaches have tried to estimate the effect of social distancing measures on COVID-19 such as [20] which uses a stochastic mass action compartmental model and [21] which used an age stratified mass action model.

We find it very difficult, however, to trust estimates of interventions aimed at breaking up contacts when the underlying assumption of how members of the population contact each other is entirely unrealistic. This mirrors the work of [22] who wrote, "realistic mixing can be an important factor to consider in order for the models to provide a reliable assessment of intervention strategies" (p.31). There is a large body of research showing how in many settings homogeneous mixing is inadequate for accurately modeling disease dynamics, such as [22–28] (see [24] and [26] for further reference listings on this). As a recent concrete example, [29] evaluated model assumptions in the West African Ebola outbreak and stated, "we see that alternative hypotheses for how EVD spreads, such as homogeneous mixing and nearest neighbor interactions, provide quantitatively poorer agreement with data" (p.3).

Individual-based models (IBMs) provide a method for capturing heterogeneous mixing. Examples of these applied to COVID-19 include [30, 31]. However, not all IBMs accurately capture realistic contact networks, such as [32] which assumes a Poisson distribution. This misses the profound impact that so-called superspreaders have on the outbreak [33, 34], and that these superspreaders "transmit infection to many other members of the population, while most infectives do not transmit infections at all or transmit infections to very few others. This suggests that homogeneous mixing at the beginning of an epidemic may not be a good approximation"([28], p.120). These IBMs, however, come at a steep computational cost and can often necessitate a large time commitment as well as a high level of expertise to design and code efficiently.

The contribution of this paper is primarily to present a computationally efficient estimation method for a network-based IBM which can be used for evaluating

nonpharmaceutical interventions such as implementing or lifting social distancing measures or implementing universal personal protective equipment (PPE). Our second contribution is to use this method to provide critical information on the effects of various nonpharmaceutical mitigation measures in Iowa at various times and to various degrees.

Methods

Overview

Our proposed method for modeling disease transmission dynamics through a susceptible-exposed-infectious-recovered (SEIR) model relies on a contact network rather than mass action assumptions. It focuses on the individuals in the population, but rather than simulating disease over an individual-based model and averaging the results to obtain an estimated epidemic curve, our method directly estimates the probability that a particular individual is infectious at a particular time. Through the use of recursive relationships, the expected number of infected individuals can be efficiently computed at each time point. Like all methods, there are strengths and weaknesses.

The strengths of the method include the following. First, it relies on a realistic or observed contact network. This is in contrast to assumptions of homogeneous mixing, or that the contact degree distribution is not heavy tailed (e.g., Poisson). This crucially allows us to capture the effects of superspreaders [33, 34], burstiness of the epidemic [35, 36], and other salient features of realistic contact graphs. Second, our approach explicitly captures the way nonpharmaceutical interventions can affect the disease transmission through quarantining/social distancing or reducing the risk that a susceptible-infective contact will lead to a new transmission through, e.g., personal protective equipment (PPE). Third, our approach is computationally efficient and can be run for even large populations with limited computing resources. Unlike many other epidemiological IBMs, our method is easily and quickly deployed (a small `R` package for implementing this methodology is provided in the supplementary material). Combining all three of these strengths, our method allows a user to quickly explore the effects of public policy changes on social distancing or universal PPE interventions, thereby providing decision makers a timely method of evaluating, for example, when and to what degree social distancing measures should be implemented or relaxed.

Our method is limited in that some disease characteristics are simplified in exchange for more accurate contact patterns and computational efficiency. Specifically, it assumes that everyone who becomes infected experiences a constant latent period and is able to transmit the disease to their set of regular contacts (either directly or through the environment) for the same amount of time. While these quantities can be estimated from the data, it does not reflect the varying lengths of time individuals are susceptible nor the varying lengths of time individuals are infectious before recovering, dying, or being effectively isolated.

Approach

We begin by presenting the setup and notation we will use. For a population of size N, let the initial probability that an individual is infected be denoted as p_0. For $j = 1, 2, \ldots, N$, let $x_{tj} = 1$ if individual j is *infective* at time t, $t = 1, 2, \ldots, T$, and 0 otherwise. The probability that $x_{tj} = 1$, $\mathbb{E}(x_{tj})$, is denoted by $\hat{x}_{tj}$. The N individuals in the population are connected through a contact graph which is represented by a $N \times N$ adjacency matrix A such that $A_{ij} = 1$ if i and j can contact each other and 0 otherwise. The probability that a susceptible individual j is infected by an infective neighbor on the contact graph at time t is denoted by p_t. If this event occurs, the susceptible enters

a latent period of D_E days where they have been exposed but are not yet infectious. This latent period is immediately followed by a period of D_I days where the individual is infective, and hence $\sum_t x_{tj} = D \; \forall j$. Let $\mathcal{I}_t$ denote the set of infectives at time t, and let $\mathcal{N}_j$ denote the neighbors of j on the contact graph. At time t, let Q_{tj} denote the event that susceptible individual j is self-quarantining, and let this event occur with probability q_{tj}. Let ι denote the daily probability of a susceptible individual importing the disease from outside the population of interest. Finally, let H_{tj} denote the event that j is successfully infected at time t (and hence will enter the latent period for D_E days), where H_{0j} corresponds to the event that j is the outbreak's initializer/patient zero.

The goal of the analysis is to estimate the expected number of new infections each day- or equivalently each day's expected cumulative number of infections- according to the individual-based model described above. To achieve this, we first focus on estimating the probability of being infective for each individual in the population on each day, i.e., $\hat{x}_{tj}$.

For the first few days of the outbreak, the only infective(s) will be the outbreak initializer(s). If the latent period is longer than the infectious period then there will be one or more days with zero infectives. If the opposite is true ($D_E < D_I$), then following these first few days there will be a period where the probability an individual is infective equals the probability that they are either the outbreak initializer or were infected within the first $t - D_E$ days. After this, the probability that an individual is infective equals the probability that they were not an initializer and were infected within a moving window such that they have passed the latent period but have not yet recovered. To put this concretely in mathematical terms, we have the following. For $1 \leq t \leq \min(D_E, D_I)$,

$$\hat{x}_{tj} = p_0. \tag{1}$$

If $D_E > D_I$, then for $D_I < t \leq D_E$,

$$\hat{x}_{tj} = 0, \tag{2}$$

else if $D_E < D_I$, then for $D_E < t \leq D_I$,

$$\hat{x}_{tj} = \text{Prob}\left(\bigcup_{s=0}^{t-D_E} H_{sj}\right). \tag{3}$$

Finally, we have for $t > \max(D_I, D_E)$,

$$\hat{x}_{tj} = \text{Prob}\left(\left\{\bigcap_{s=0}^{\max(0,t-D_E-D_I)} H'_{sj}\right\} \cap \left\{\bigcup_{s=\max(1,t-D_E-D_i+1)}^{t-D_E} H_{sj}\right\}\right). \tag{4}$$

If individual j is still susceptible at time t, they can become infected by either importing the disease from outside of the study population or by being infected by an infective neighbor on the contact graph. This latter method requires both that j is not quarantined at time t and that at least one infective neighbor infects j. Hence by the law of total expectation we have that

$$\begin{aligned}
\text{Prob}\left(H_{tj} \middle| \bigcap_{s<t} H'_{sj}\right) &= \iota + (1-\iota)(1-q_{tj})\Big(1 - \mathbb{E}(\text{Prob}(\text{no infectives infect } j | Q'_{sj}, \boldsymbol{x}_t)\Big) \\
&= \iota + (1-\iota)(1-q_{tj})\left(1 - \mathbb{E}\left(\prod_{i \in \mathcal{N}_j \cap \mathcal{I}_t} (1-p_t)\right)\right) \\
&= \iota + (1-\iota)(1-q_{tj})\left(1 - \mathbb{E}\left((1-p_t)^{\boldsymbol{x}'_t A_{\cdot j}}\right)\right),
\end{aligned}$$

where $\boldsymbol{x}_t = (x_{t1}, x_{t2}, \ldots, x_{tN})'$ and $A_{\cdot j}$ is the j^{th} column of the adjacency matrix A. Using a first order Taylor's expansion around $\hat{\boldsymbol{x}}_t$, we have

$$\begin{aligned}
&\text{Prob}\left(H_{tj}\Big|\bigcap_{s<t} H'_{sj}\right)\\
&\approx \iota + (1-\iota)(1-q_{tj})\left(1 - \mathbb{E}\left((1-p)^{\hat{\boldsymbol{x}}_t' A_{\cdot j}} + (\boldsymbol{x}_t - \hat{\boldsymbol{x}}_t)'\nabla\left\{(1-p_t)^{\boldsymbol{x}_t' A_{\cdot j}}\right\}\Big|_{\boldsymbol{x}_t=\hat{\boldsymbol{x}}_t}\right)\right),\\
&= \iota + (1-\iota)(1-q_{tj})\left(1-(1-p)^{\hat{\boldsymbol{x}}_t' A_{\cdot j}}\right), \qquad (5)
\end{aligned}$$

or equivalently

$$\text{Prob}\left(H'_{tj}\Big|\bigcap_{s<t} H'_{sj}\right) \approx (1-\iota)\left(q_t + (1-q_t)(1-p_t)^{\hat{\boldsymbol{x}}_t' A_{\cdot j}}\right). \qquad (6)$$

For ease of notation, we let this quantity in (6) be notated as f_{tj}.

Combining Eq (1)-(6) yields the following.

$$\begin{aligned}
1 < t \le \min(D_E, D_I), \quad & \hat{x}_{tj} = p_0,\\
\min(D_E, D_I) < t \le \max(D_E, D_I), \quad & \hat{x}_{tj} = \begin{cases} 1-(1-p_0)\prod_{s=1}^{t-D_E} f_{sj} & \text{if } D_E < D_I \\ 0 & \text{if } D_E > D_I \end{cases}\\
t > \max(D_E, D_I) \quad & \hat{x}_{tj} = \alpha_{\max(0,t-D_E-D_I)j}\left(1 - \prod_{s=\max(1,t-D_E-D_i+1)}^{t-D_E} f_{sj}\right).
\end{aligned} \qquad (7)$$

Here α_{tj} is defined to be the probability that individual j is still susceptible by time t. These quantities can be computed recursively in the following manner. First, $\alpha_{0j} := \text{Prob}(H'_{0j}) = 1 - p_0$. Subsequently for $t > 0$ we have

$$\alpha_{tj} := \text{Prob}\left(\bigcap_{s=0}^{t} H'_{sj}\right) = \alpha_{(t-1)j} f_{tj}. \qquad (8)$$

These recursions then allow us to compute the quantity of interest, namely the number of infections we expect to have by time t. This is derived from the expected number of susceptible individuals:

$$\begin{aligned}
\mathbb{E}(\#\text{ infected}) &= \text{Pop. size } - \mathbb{E}(\#\text{ susceptible})\\
&= N - \sum_{j=1}^{N} \alpha_{tj}. \qquad (9)
\end{aligned}$$

The parameters to be estimated include the length of the disease's latent period (D_E), the number of days an individual is infective (D_I), the probabilities that a contact leads to a transmission event (p_t), and the probabilities that an individual is quarantined at time t (q_t). The initial probability p_0 may also need to be estimated, but in many cases this will be a known (small) number, such as $1/N$ for a single initializer. Given a contact graph, prior to social distancing and any intervention which may affect transmission probabilities the quantities p_t may be related to the more intuitive reproduction number, or R_0, defined to be the expected number of new infections generated by a given infective. This can be computed as

$R_0 = (\#\text{ days infectious}) \times \mathbb{E}(\#\text{ contacts per day}) \times \text{Prob(S-I contact leads to new transmission)}$

and hence

$$p_t = \frac{R_0}{D\bar{d}}, \tag{10}$$

where $\bar{d}$ is the average degree in the contact graph A, i.e., the average number of neighbors in A. Estimation can be performed via ordinary least squares (OLS), i.e., minimizing the sum of squared differences between the observed and the expected number of daily cases.

COVID-19 in Iowa

Case Data

We used publicly available data collected by The COVID Tracking Project [37] for the state of Iowa. This data source provides the daily number of lab confirmed cases which we used to train our IBM. We used recent results from a study involving a random sample of individuals to test in Indiana [38] which estimated the infection fatality rate (IFR) to be 0.58%. This IFR was then used to scale the number of positive cases with the number of estimated cases based on the total deaths in Iowa.

Contact graph

[39] recruited 1450 individuals from 857 households in Hong Kong into a study on inter-personal contacts, where a contact was defined to be a social encounter which included a "face-to-face conversation or touch (such as handshake, a kiss, games and sports or similar events involving body touch)." As was consistent with other studies, [39] found the distribution of contacts to be heavy tailed, which has profound effects in the context of infectious disease as this indicates potential super-spreaders. Overall, individuals had on average 12.5 contacts per day. This matches closely with an ecological momentary assessment study of individuals in upstate New York which found the average number of daily contacts to be 12 [40]. We therefore constructed a contact graph for the ~ 3.155M Iowans with a degree distribution which resembled that of [39].

Mobility data

Google Community Mobility Reports [41] used geolocated mobile phone data to assess various populations' movement patterns. This was measured by first capturing a baseline rate of movement and then evaluating deviations from this baseline rate. These baseline measurements were taken from the period 3 January, 2020 - 6, February, 2020, and were broken down by day of the week and by category (workplace, retail and recreation, etc.). We chose to focus on the category of retail and recreation, as this seemed to best reflect voluntary movement patterns. When we performed estimation, we included a parameter which scaled these deviations from baseline to obtain a daily estimate of the probability an individual would self-quarantine.

Seasonality

Seasonality can potentially play a large role in the transmission pattern of COVID-19, and "epidemiological data on seasonal [coronavirsues] may provide valuable information about individuals and seasonal conditions favoured by, or limiting, an invading CoV" ([42], p. 1). We used data collected in Michigan, USA, by [43] to estimate relative risks of infection of human coronaviruses (HCoVs). The four known HCoVs display a striking similarity in seasonal patterns, and we assume here that SARS-CoV-2 will show similar patterns. To estimate relative risks, we first obtained the number of infections per

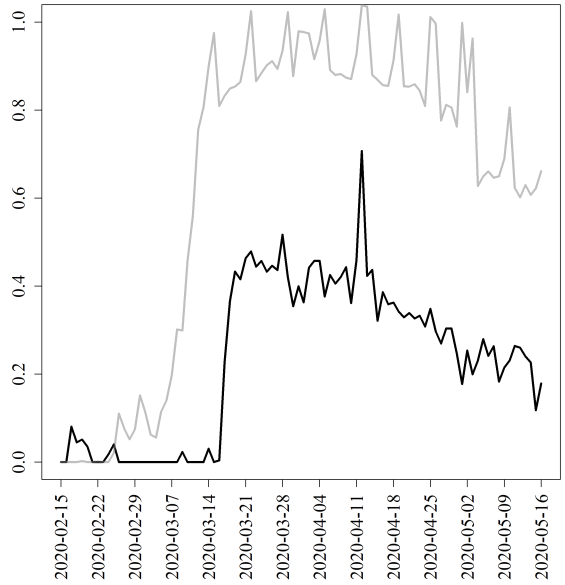

Fig 1. Estimated levels of quarantining based on the Google Community Mobility Reports. The values in these reports have been scaled by a quantity estimated by training our IBM.

month aggregated over all coronaviruses in their study. We then used a Bayesian approach to estimate the relative risks by using the posterior mean with a uniform prior over the probabilities that a HCoV infection would occur in a particular month. We then smoothed these estimated monthly relative risks across 365 days. In this way our model estimated a single transmission probability and then adjusted daily transmission probabilities according to the daily relative risks.

Scenarios

We trained our model on the available data and used this to project into the future under several scenarios. We first computed projections for maintaining the current (as of May 25, 2020) estimated level of social distancing/self-quarantining without any modifications. Second, we computed forecasts for relaxing social distancing measures entirely as of May 25, 2020. Since this relaxation is not likely to occur immediately, we set the quarantine probability to decay according to a Gaussian kernel such that after one week the current levels of social distancing levels were reduced by 90%. Knowing that a second peak is forecasted to come in the late fall, we estimated the effects of reimplementing on October 1st, November 1st, or December 1st social distancing at the maximum observed level of social distancing in Iowa[1] as well as at the average level of social distancing observed in Italy for the 30 days following March 12, 2020. This was chosen as an estimate for how strongly Iowa might respond to a dramatic public health crisis. Figure 1 shows the estimated levels of quarantining based on the Google Community Mobility Reports and the IBM.

We further estimated the effects of reimplementing social distancing for only a strategic portion of the population. This was determined by implementing social distancing for those individuals with the highest number of contacts (e.g., healthcare professionals rotating between long term care facilities) while maintaining no social

[1]Excluding a severe drop in activity on April 12, 2020 (Easter).

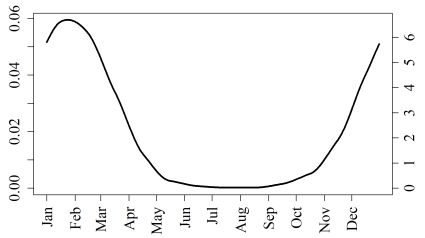

Fig 2. Seasonal transmission dynamics. Left: transmission probability for a susceptible-infective contact. Right: Basic R_0.

distancing measures for the remainder of the population.

Finally, we evaluated the effects of reducing the transmission probability. This could be accomplished through, for example, universally requiring personal protective equipment.

Results

By May 25, 2020, we had records of 454 deaths in Iowa due to COVID-19 infections and 17,252 lab confirmed cases. Figure 3 shows the observed daily and cumulative case counts data alongside the estimated expected number of confirmed cases. In the plot of daily cases, the estimated transmission probability is also given. At the beginning of the epidemic in Iowa we estimated an R_0 of 4.6; due to assumed seasonality, this ranged over the course of the year, and these seasonal dynamics are given in Figure 2. The latent period was estimated to be 4 days, which is in line with previous estimates [18, 44]. The infectious period was estimated to be 9 days, and the daily probability of an individual importing COVID-19 from outside of the population was estimated to be 4.5×10^{-6}.

Figures 4 to 6 show the main results for projecting under various mitigation measures. Each of these three figures corresponds to a given starting date (October 1, November 1, or December 1), and in all cases the current trajectory, as determined by the estimated level of quarantining as of May 25, 2020, is given in black, while the trajectory corresponding to permanently relaxing the current level of quarantining is given in gray. Each plot shows projections in green for reimplementing quarantining measures for either individuals with the top 10% of contacts, with the top 50% of contacts, or for all individuals. The columns show when the reimplemented quarantining level was set to either be the maximum level observed in Iowa or the higher level observed in Italy during the height of their public health crisis. Finally, the rows show the absence/presence of attempts to reduce the transmission probability. The strong attempt was set at reducing the transmission probability by 90%. While this may seem very strong at first blush, this comes from observed rates of droplet containment for face shields. Specifically, [45] found that face shields reduced inhalation exposure from a influenza-laden cough aerosol by the wearer by 96% and for smaller droplets by 68%. If we use the more conservative value and assume that this reduction rate holds for both the infected and susceptible, this leads to a reduction of $1 - (1 - 0.68)^2 = 0.90$.

Discussion

There are several key takeaways from our analysis of COVID-19 in Iowa. First, the current level of self-quarantining is estimated to be at a sufficiently low level as to make a surprisingly low impact on the disease curve, and in the period between the first and

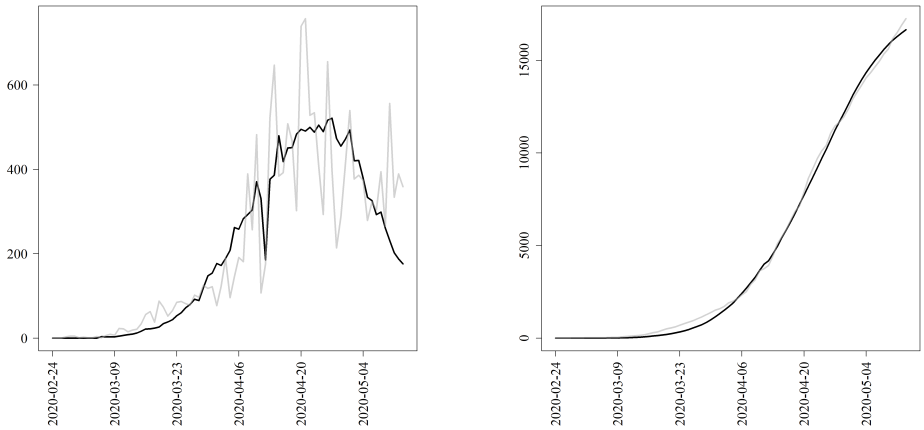

Fig 3. Fitting the individual-based model (black solid) to the daily (left) and cumulative (right) number of confirmed infections (gray solid).

second peak, the differences between quarantining at the current level and not quarantining are negligible. The impact of Iowa's current low level of self-quarantining is dominated by the overwhelming transmission patterns that will emerge in the late fall. This pattern and how it dwarfs the initial peak is perhaps not unsurprising when one considers that the first peak in Iowa began in March after the seasonal transmission of HCoVs begins to decline, and for the duration of the high HCoV season, COVID-19 needed to percolate throughout the population before being capable of driving the epicurve upwards. In contrast, by the time the second peak begins, COVID-19 will have dispersed thoroughly throughout the population while only having infected less than 3% of the population, and thus will be in a position to have maximal impact as the high HCoV season begins.

Second, without additional attempts at reducing the transmissibility, a high level of quarantining is insufficient to keep the second peak at a manageable level. Even if quarantining is applied the same across the entire population at the strongest observed quarantining levels in Iowa of the spring of 2020, these measures are insufficient to preclude the epidemic from reaching catastrophic levels, nor does applying the much stronger levels observed in Italy prove to be insufficient.

Third, reducing the transmission probability through universal PPE, behavioral changes, or some other mechanism appears to be the strongest pathway for controlling the second peak. Indeed, these results indicate that pairing transmission reduction with quarantining only the top 10% of individuals based on number of contacts and quarantining them at the Iowan rather than Italian rate, the second peak could be very minimal.

Finally, timing will be crucial. We forecast that the number of daily cases will be extremely small (< 20/day) for late summer and early fall, but starting around October daily cases could pick up at a very rapid rate. Thus if transmission probabilities can be reduced at or prior to October, the second peak will be minimal, while waiting until December could lead to a dramatic number of infections quickly leading to an overburdened healthcare system.

This analysis has made the strong assumption that SARS-CoV-2 will exhibit the same seasonal trends as other coronaviruses. While this assumption appears to fit the data well, there is a dire need for more research into the presence/absence of seasonality of COVID-19. One other possibility that may explain the recent downward trajectory in Iowa is that individuals' behaviors have reduced the transmissibility. This could be due

to an increasing number of individuals wearing face masks in public, precautions taken by retailers to sanitize surfaces and protect employees, etc. However, to the authors' knowledge there is no existing data source for measuring such a reduction in transmissibility due to individuals' behaviors, and hence the results presented here need to be read with this limitation in mind. That is, if the observed reduction in transmissibility is due to behaviors rather than seasonality, then we would not expect COVID-19 to resurge with such strength in the late fall/early winter of 2020. Nevertheless, these results showcase the effects of various mitigation measures that could be taken should a second peak begin to appear due to either seasonality or other causes such as university and school openings in the fall.

Conclusion

In an ongoing outbreak, data streams are being continually updated, and estimates of the disease trajectory are highly dynamic. Data and estimates quickly become outdated, and hence it is necessary to be able to provide accurate forecasts and projections of intervention effects rapidly. Our approach provides an analytically tractable solution to compute the expected epidemic curve. Our approach is thus inherently fast and computationally inexpensive compared to simulation-based inference. This is crucial when decision makers need to see a myriad of scenarios of implementing or ceasing nonpharmaceutical interventions. In addition, simulation-based inference can only approximate the expected epidemic curve, while our approach yields an exact solution. Moreover, this is accomplished while maintaining high fidelity transmission patterns through the use of contact graphs.

References

1. Zhu N, Zhang D, Wang W, Li X, Yang B, Song J, et al. A novel coronavirus from patients with pneumonia in China, 2019. New England Journal of Medicine. 2020;382(8):727–733.

2. Chen N, Zhou M, Dong X, Qu J, Gong F, Han Y, et al. Epidemiological and clinical characteristics of 99 cases of 2019 novel coronavirus pneumonia in Wuhan, China: a descriptive study. The Lancet. 2020;395(10223):507 – 513.

3. Wang D, Hu B, Hu C, Zhu F, Liu X, Zhang J, et al. Clinical characteristics of 138 hospitalized patients with 2019 novel coronavirus infected pneumonia in Wuhan, China. JAMA. 2020;323(11):1061–1069.

4. Richardson S, Hirsch JS, Narasimhan M, Crawford JM, McGinn T, Davidson KW, et al. Presenting characteristics, comorbidities, and outcomes among 5700 patients hospitalized with COVID-19 in the New York City area. JAMA. 2020;doi:10.1001/jama.2020.6775.

5. Dong E, Du H, Gardner L. An interactive web-based dashboard to track COVID-19 in real time. The Lancet Infectious Diseases. 2020;20(5):533 – 534. doi:https://doi.org/10.1016/S1473-3099(20)30120-1.

6. Murray CJ. Forecasting the impact of the first wave of the COVID-19 pandemic on hospital demand and deaths for the USA and European Economic Area countries. medRxiv. 2020;doi:10.1101/2020.04.21.20074732.

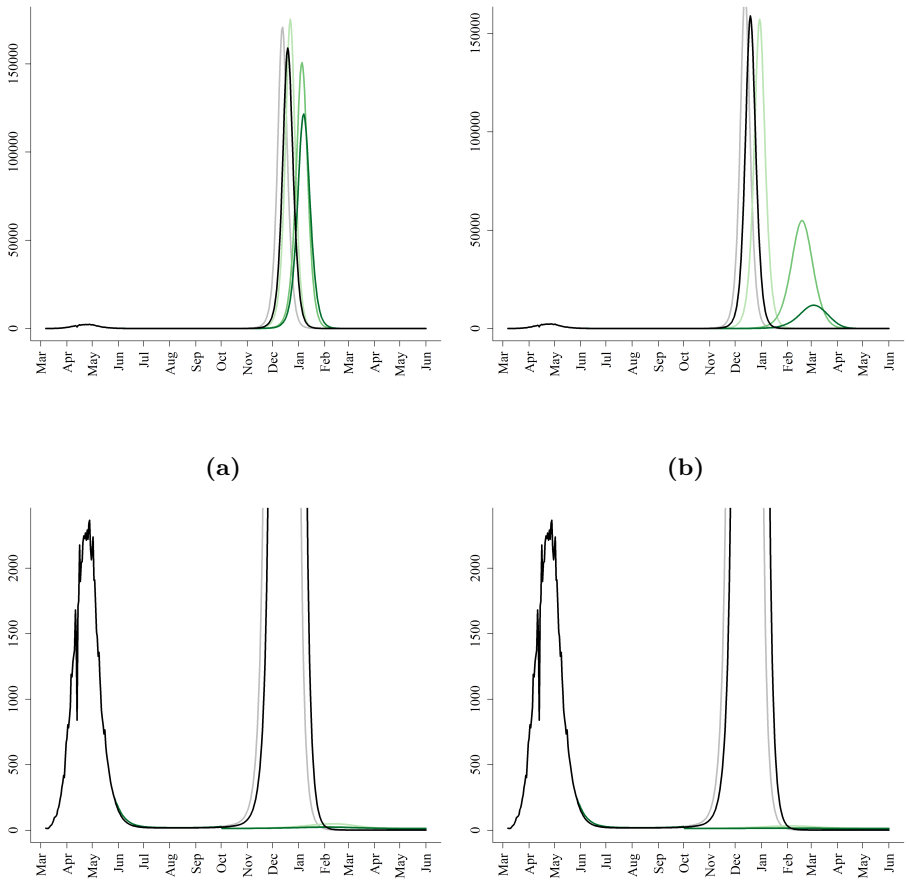

Fig 4. Iowa COVID-19 projections for various mitigation strategies starting on October 1. The estimated current trajectory is given in black curves, and the trajectory after permanently relaxing quarantining on May 25, 2020, is given in gray. The green curves show projections for reimplementing social distancing for individuals with the top 10% of contacts (light), 50% (medium), or for all individuals (dark). The top (bottom) row corresponds to no (strong) attempts at reducing transmission probabilities. The left (right) column corresponds to quarantining rates at the previous Iowan (Italian) levels.

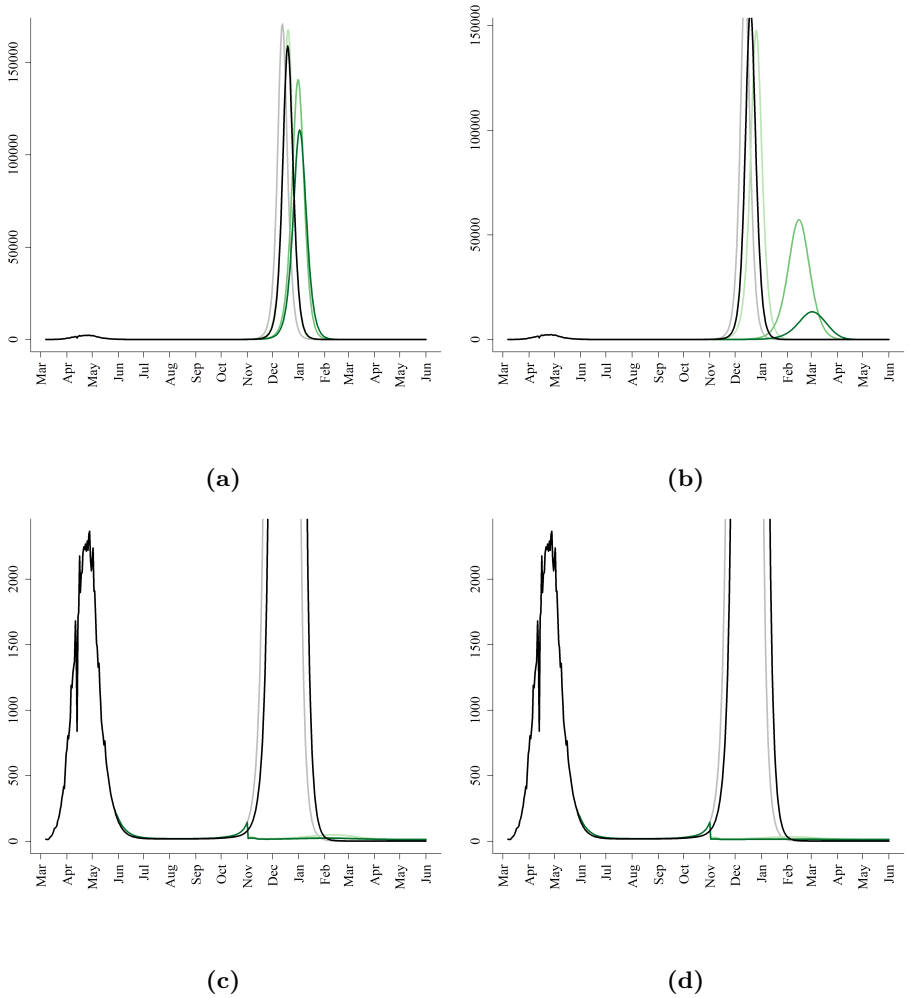

Fig 5. Iowa COVID-19 projections for various mitigation strategies starting on November 1. The estimated current trajectory is given in black curves, and the trajectory after permanently relaxing quarantining on May 25, 2020, is given in gray. The green curves show projections for reimplementing social distancing for individuals with the top 10% of contacts (light), 50% (medium), or for all individuals (dark). The top (bottom) row corresponds to no (strong) attempts at reducing transmission probabilities. The left (right) column corresponds to quarantining rates at the previous Iowan (Italian) levels.

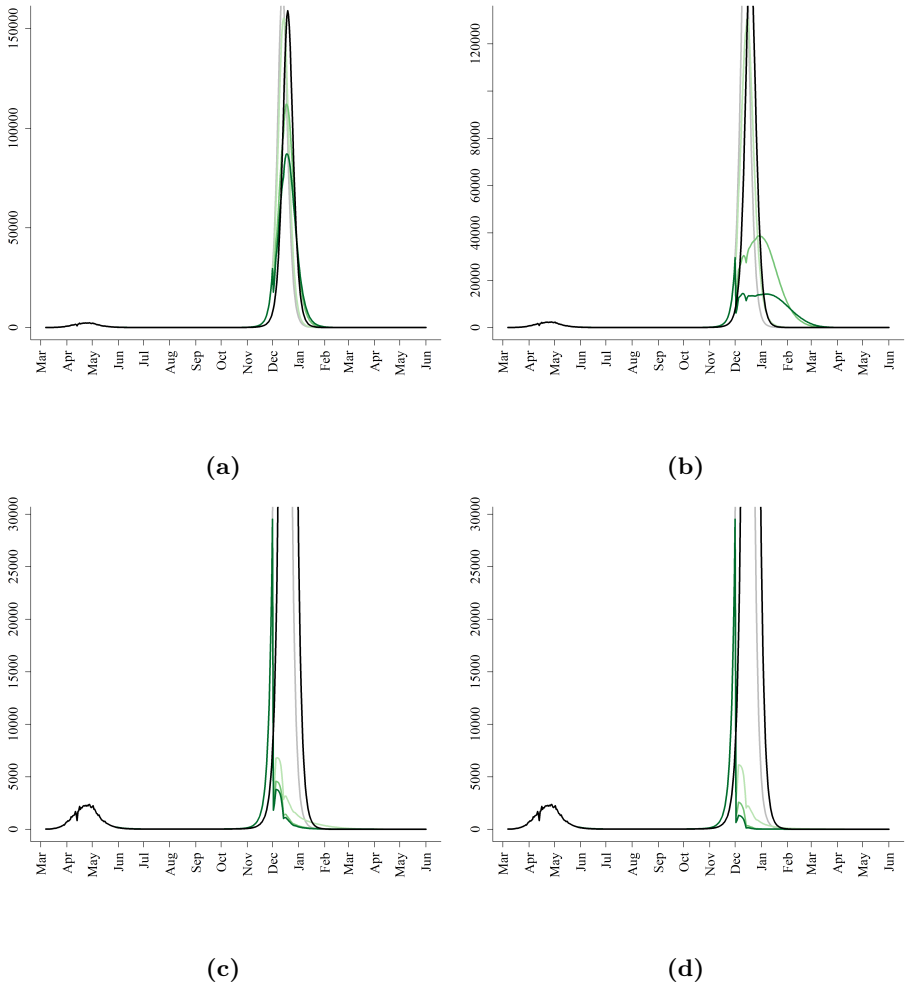

Fig 6. Iowa COVID-19 projections for various mitigation strategies starting on December 1. The estimated current trajectory is given in black curves, and the trajectory after permanently relaxing quarantining on May 25, 2020, is given in gray. The green curves show projections for reimplementing social distancing for individuals with the top 10% of contacts (light), 50% (medium), or for all individuals (dark). The top (bottom) row corresponds to no (strong) attempts at reducing transmission probabilities. The left (right) column corresponds to quarantining rates at the previous Iowan (Italian) levels.

7. Anastassopoulou C, Russo L, Tsakris A, Siettos C. Data-based analysis, modelling and forecasting of the COVID-19 outbreak. PLOS ONE. 2020;15(3):1–21. doi:10.1371/journal.pone.0230405.

8. Neher R, Aksamentov I, Noll N, Albert H, Dyrdak R. COVID-19 Scenarios; Accessed 27 April, 2020.

9. Weissman GE, Crane-Droesch A, Chivers C, Luong T, Hanish A, Levy MZ, et al. Locally Informed Simulation to Predict Hospital Capacity Needs During the COVID-19 Pandemic. Annals of Internal Medicine. 2020;doi:10.7326/M20-1260.

10. Sen Pei JS. Initial simulation of SARS-CoV2 spread and intervention effects in the continental US. medRxiv. 2020;doi:10.1101/2020.03.21.20040303.

11. Branas CC, Rundle A, Pei S, Yang W, Carr BG, Sims S, et al. Flattening the curve before it flattens us: hospital critical care capacity limits and mortality from novel coronavirus (SARS-CoV2) cases in US counties. medRxiv. 2020;doi:10.1101/2020.04.01.20049759.

12. Imperial College London: Short-term forecasts of COVID-19 deaths in multiple countries;. `https://mrc-ide.github.io/covid19-short-term-forecasts/index.html`.

13. Los Alamos National Laboratory: COVID-19 Confirmed and Forecasted Case Data;. `https://covid-19.bsvgateway.org`.

14. Woody S, Garcia Tec M, Dahan M, Gaither K, Lachmann M, Fox S, et al. Projections for first-wave COVID-19 deaths across the US using social-distancing measures derived from mobile phones. medRxiv. 2020;doi:10.1101/2020.04.16.20068163.

15. COVID Analytics: DELPHI Epidemiological Case Predictions;. `https://www.covidanalytics.io/projections`.

16. Kim Reynolds. Iowa Gov. Kim Reynolds Press Conference — April 1, 2020, 2:30 p.m.; 2020. URL: `https://www.youtube.com/watch?v=LVyCHyTjNOU`.

17. https://www politico com/news/2020/04/28/death-toll-coronavirus-estimate 214339; Accessed April 28, 2020.

18. Li R, Pei S, Chen B, Song Y, Zhang T, Yang W, et al. Substantial undocumented infection facilitates the rapid dissemination of novel coronavirus (SARS-CoV-2). Science. 2020;368(6490):489–493. doi:10.1126/science.abb3221.

19. Kucharski AJ, Russell TW, Diamond C, Liu Y, Edmunds J, Funk S, et al. Early dynamics of transmission and control of COVID-19: a mathematical modelling study. The Lancet Infectious Diseases. 2020;20(5):553 – 558. doi:https://doi.org/10.1016/S1473-3099(20)30144-4.

20. Song PX, Wang L, Zhou Y, He J, Zhu B, Wang F, et al. An epidemiological forecast model and software assessing interventions on COVID-19 epidemic in China. medRxiv. 2020;doi:10.1101/2020.02.29.20029421.

21. Moghadas SM, Shoukat A, Fitzpatrick MC, Wells CR, Sah P, Pandey A, et al. Projecting hospital utilization during the COVID-19 outbreaks in the United States. Proceedings of the National Academy of Sciences. 2020;117(16):9122–9126. doi:10.1073/pnas.2004064117.

22. Cui J, Zhang Y, Feng Z. Influence of non-homogeneous mixing on final epidemic size in a meta-population model. Journal of Biological Dynamics. 2019;13(sup1):31–46. doi:10.1080/17513758.2018.1484186.

23. Bansal S, Grenfell BT, Meyers LA. When individual behaviour matters: homogeneous and network models in epidemiology. Journal of the Royal Society Interface. 2007;4:879–891.

24. Del Valle SY, Hyman JM, Chitnis N. Mathematical models of contact patterns between age groups for predicting the spread of infectious diseases. Mathematical Biosciences and Engineering. 2013;10(5-6):1475–1497.

25. Feng Z, Hill AN, Smith PJ, Glasser JW. An elaboration of theory about preventing outbreaks in homogeneous populations to include heterogeneity or preferential mixing. Journal of Theoretical Biology. 2015;386:177 – 187. doi:https://doi.org/10.1016/j.jtbi.2015.09.006.

26. Bioglio L, Génois M, Vestergaard CL, Poletto C, Barrat A, Colizza V. Recalibrating disease parameters for increasing realism in modeling epidemics in closed settings. BMC Infectious Diseases. 2016;16:676.

27. Chowell G, Sattenspiel L, Bansal S, Viboud C. Mathematical models to characterize early epidemic growth: A review. Physics of Life Reviews. 2016;18:66 – 97. doi:https://doi.org/10.1016/j.plrev.2016.07.005.

28. Brauer F. Mathematical epidemiology: Past, present, and future. Infectious Disease Modelling. 2017;2(2):113 – 127. doi:https://doi.org/10.1016/j.idm.2017.02.001.

29. Burghardt K, Verzijl C, Huang J, Ingram M, Song B, Hasne MP. Testing modeling assumptions in the West Africa Ebola outbreak. Scientific Reports. 2016;6:34598.

30. Shoukat A, Wells CR, Langley JM, Singer BH, Galvani AP, Moghadas SM. Projecting demand for critical care beds during COVID-19 outbreaks in Canada. CMAJ. 2020;doi:10.1503/cmaj.200457.

31. Ferguson N, Laydon D, Nedjati Gilani G, Imai N, Ainslie K, Baguelin M, et al. Report 9: Impact of non-pharmaceutical interventions (NPIs) to reduce COVID19 mortality and healthcare demand. 2020;.

32. Kerr CC MDARHGRRSPNRHBGLIAPADDBCWBCSCJPGJJMOAWEFMKD Stuart RM. Covasim: an agent-based model of COVID-19 dynamics and interventions. 2020;.

33. Stein RA. Super-spreaders in infectious diseases. International Journal of Infectious Diseases. 2011;15(8):e510 – e513. doi:https://doi.org/10.1016/j.ijid.2010.06.020.

34. Hornbeck T, Naylor D, Segre AM, Thomas G, Herman T, Polgreen PM. Using sensor networks to study the effect of peripatetic healthcare workers on the spread of hospital-associated infections. The Journal of Infectious Diseases. 2012;206(10):1549–1557. doi:10.1093/infdis/jis542.

35. Karsai M, Kivelä M, Pan RK, Kaski K, Kertész J, Barabási AL, et al. Small but slow world: How network topology and burstiness slow down spreading. Phys Rev E. 2011;83:025102. doi:10.1103/PhysRevE.83.025102.

36. Colman ER, Vukadinovi ć Greetham D. Memory and burstiness in dynamic networks. Phys Rev E. 2015;92:012817. doi:10.1103/PhysRevE.92.012817.

37. Project TCT. https://covidtracking.com/;.

38. Zeek A, Briggs A. IU, ISDH release preliminary findings about impact of COVID-19 in Indiana;. https://news.iu.edu/stories/2020/05/iupui/releases/13-preliminary-findings-impact-covid-19-indiana-coronavirus.html.

39. Kwok KO, Cowling B, Wei V, Riley S, Read JM. Temporal variation of human encounters and the number of locations in which they occur: a longitudinal study of Hong Kong residents. Journal of The Royal Society Interface. 2018;15(138):20170838.

40. Zhaoyang R, Sliwinski MJ, Martire LM, Smyth JM. Age differences in adults' daily social interactions: An ecological momentary assessment study. Psychology and Aging. 2018;33(4):607–618.

41. Aktay A, Bavadekar S, Cossoul G, Davis J, Desfontaines D, Fabrikant A, et al. Google COVID-19 community mobility reports: Anonymization process description (version 1.0). arXiv preprint arXiv:200404145. 2020;.

42. Nickbakhsh S, Ho A, Marques DFP, McMenamin J, Gunson RN, Murcia PR. Epidemiology of Seasonal Coronaviruses: Establishing the Context for the Emergence of Coronavirus Disease 2019. The Journal of Infectious Diseases. 2020;doi:10.1093/infdis/jiaa185.

43. Monto AS, DeJonge PM, Callear AP, Bazzi LA, Capriola SB, Malosh RE, et al. Coronavirus Occurrence and Transmission Over 8 Years in the HIVE Cohort of Households in Michigan. The Journal of Infectious Diseases. 2020;doi:10.1093/infdis/jiaa161.

44. Sanche S, Lin YT, Xu C, Romero-Severson E, Hengartner N, Ke R. High contagiousness and rapid spread of Severe Acute Respiratory Syndrome Coronavirus 2. Emerging Infectious Diseases. 2020;26(7).

45. Lindsley WG, Noti JD, Blachere FM, Szalajda JV, Beezhold DH. Efficacy of face shields against cough aerosol droplets from a cough simulator. Journal of Occupational and Environmental Hygiene. 2014;11(8):509–518. doi:10.1080/15459624.2013.877591.